

Strong anti-kinetoplastid activity of silver nanoparticle-coated biochar

Youssef Snoussi¹, Inès Sifaoui^{2,3,4,5}, Ahmed M. Khalil^{6,7}, Arvind K. Bhakta^{1,8}, Laurent Michely⁷, Rémy Pires⁷, Stéphane Bastide⁷, Oleg Semyonov⁹, Pavel S. Postnikov⁹, José Enrique-Piñero Barroso^{2,3,4,5}, Jacob Lorenzo Morales^{2,3,4,5,*}, Mohamed M. Chehimi^{1,7,*}

¹ Université de Paris, CNRS, ITODYS (UMR 7086), 75013 Paris, France

² Instituto Universitario de Enfermedades Tropicales y Salud Pública de Canarias, Universidad de La Laguna, Avda. Astrofísico Fco. Sánchez, S/N, La Laguna, Tenerife, 38203, Islas Canarias, Spain

³ Departamento de Obstetricia, Ginecología, Pediatría, Medicina Preventiva y Salud Pública, Toxicología, Medicina Legal y Forense y Parasitología, Universidad de la Laguna (ULL), La Laguna, Tenerife, 38203 Islas Canarias, Spain

⁴ Red de Investigación Cooperativa en Enfermedades Tropicales (RICET), 28029 Madrid, Spain

⁵ CIBER de Enfermedades Infecciosas (CIBERINFEC), Instituto de Salud Carlos III, 28029 Madrid, Spain

⁶ Photochemistry Department, National Research Centre, Dokki, Giza 12622, Egypt

⁷ Université Paris Est, CNRS, ICMPE (UMR 7182), 94320 Thiais, France

⁸ Department of Chemistry, St. Joseph's College, Lalbagh Road, Bangalore, Karnataka, 560 027, India

⁹ Tomsk Polytechnic University, 634050 Tomsk, Russian Federation

Abstract

Neglected tropical diseases including Chagas disease, also known as American trypanosomiasis and leishmaniasis remains a serious health problem in several endemic. To address this medical problem, much has been done in the past 15 years to design nanomaterials with effective anti-kinetoplastids activity, particularly those nanomaterials based on gold and silver nanoparticles. Herein, we describe a simple method to prepare silver-loaded biochar by pyrolysis of silver nitrate-impregnated agrowaste powder (from olive stones). The resulting Biochar@Ag was prepared at 400 °C for 15 minutes only and the yield was found to be 36.5 %. The supported metallic Ag nanoparticles have triangular shape in the nanoscale regime (< 100 nm) and a loading of 7.85 mmol per gram of Biochar@Ag. The Biochar@Ag showed promising antiparasitic activity against promastigotes stage of *L. donovani*, *L. amazonensis* and epimastigotes of *T. cruzi* with and IC₅₀ of 9.942 ± 0.900 ppm; 14.555 ± 1.035 ppm and 12.154 ± 0.206 ppm, respectively. From the above, this work conclusively demonstrates that slow pyrolysis is a unique thermochemical approach to valorize agrowastes into highly effective anti-kinetoplastid silver-loaded biochar with remarkably low cytotoxicity towards murine macrophages.

Keywords:

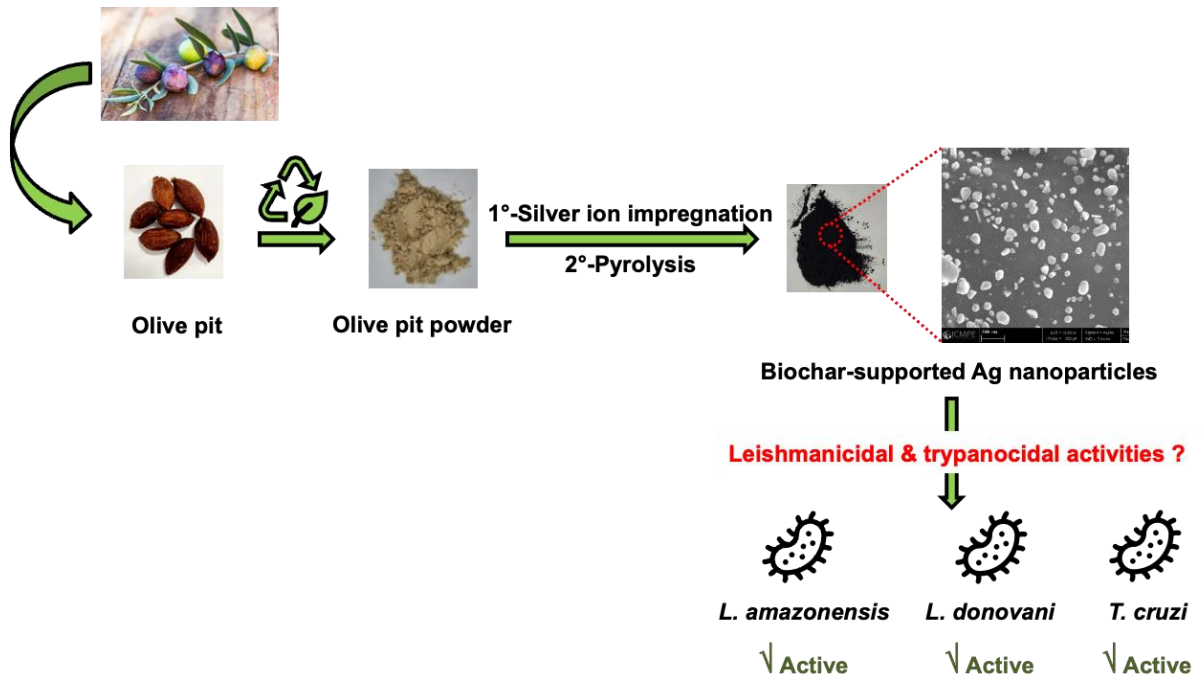
Leishmania; neglected tropical disease; antiparasitic nanocomposite; agrowaste; olive pit; biochar; silver nanoparticles; trash to treasure.

Corresponding authors

Jacob Lorenzo Morales: jmlorenz@ull.edu.es ;

Mohamed M. Chehimi: mohamed.chehimi@cnrs.fr

Graphical Abstract



Research Highlights

- Olive pit-derived biochar bearing silver nanoparticles has been prepared by one step slow pyrolysis
- Silver nanoparticles are densely and evenly dispersed over biochar particles
- Silver-loaded biochar has antiparasitic activity against *L. donovani*, *L. amazonensis* and *T.cruzi*.
- Waste and junk conversion to bioactive nanocomposite opens new horizons in treating neglected tropical diseases.

Introduction

Neglected Parasitic infection caused by kinetoplastids, a group of flagellated protozoans including *Leishmania* and *Trypanosoma* species, affect millions of persons and are responsible for high mortality, disability and morbidity rates [1, 2]. Leishmaniasis is considered as one of the major protozoan disease-causing high morbidities throughout the world. This infection is caused by a protist parasite of the genus *Leishmania* through the bite of a female phlebotomine sand fly [3]. Based on its clinical symptoms Leishmaniasis is classified in 3 different forms namely cutaneous, mucocutaneous and visceral leishmaniasis. As for Chagas disease (American trypanosomiasis), is caused by a protist parasite of the species *Trypanosoma cruzi* (*T. cruzi*) and is transmitted by the faeces of an hematophagous insects of the subfamily Triatominae [3]. This disease is classified into acute and chronic phases [4]. According to World Health Organization (WHO) 6 to 7 million people worldwide are estimated to be infected with *Trypanosoma cruzi* [5]. The actual treatment for those diseases is characterized by variable efficacy among different species, high toxicity and high cost resulting the urgent need for alternative anti-kinetoplastid agents. Metallic Silver (Ag), ions and their composites and compounds are well known to exhibit antiviral, antileishmanial and antibacterial activity [6]. There are numerous examples in the literature for antileishmanial applications using Ag such as the use of Chitosan-based Ag nanoparticles [7], Au_{core}@Ag_{shell} nanoparticles [8], meglumine antimoniate-TiO₂@Ag nanoparticle [9], gold-silver bimetallic nanoparticles [10] and Ag compound with imidazolidine-2-thione [11], to name but a few. Comparative studies using different NPs have found the following antileishmanial activity: Ag>Au>TiO₂>ZnO>MgO. Further, their activity is enhanced by infrared and UV light [12]. Ag NPs produced with the help of olive and fig extract are more efficient than standard drug Pentostam [13].

There are limited reports on carbonaceous based materials for anti-kinetoplastid application and out of which they are mostly utilising functionalized carbon nanotubes (CNT), graphene and CNT-graphene [14]. In the context of “trash to treasure” or “waste to wealth”, there has been an effort to synthesize Ag NPs with nanoxylan (xylan from corn cobs as a stabilizing and reducing agent) for antifungal and antileishmanial application [15]. In order to overcome the problem of silver resistance [16] and for biomass waste valorization purpose, biochar (“green carbon”) having biocompatibility [17] is a perfect candidate in association with Ag NPs for antileishmanial applications. To the best of our knowledge, there are no reports on biochar with loaded silver nanoparticles for such application.

Herein we report on novel silver-loaded biochar (Biochar@Ag) composite prepared by slow pyrolysis of olive stone agrowaste powder impregnated with silver nitrate. The resulting Biochar@Ag was characterized by XRD, SEM/EDX, TGA and XPS and its antiparasitic activity was evaluated against promastigotes stage of *Leishmania donovani*, *Leishmani amazonensis* and epimastigotes of *Trypanosoma cruzi*. The cytotoxicity towards host cells, murine macrophage, was also studied. All assays were conducted in vitro using the alamarBlue® method.

2. Experimental

2.1. Fabrication of Biochar@Ag by slow pyrolysis

Olive stone powder (3.67 g) was impregnated with an ethylic solution of silver nitrate (Aldrich, 584 mg, ~3.44 mmol in 10 mL ethanol) and left to dry. The powder was mixed from time to time on a glass lens and dried at RT until no more change in weight of the uimpregnated powder was noted. 1.2 g of AgNO₃-impregnated olive stone powder was pyrolyzed in a tubular furnace (Thermolyne, model 21100) at 400 °C for 15 min, under a stream of N₂/H₂ (95/5%) mixture. The temperature ramp was 30 °C/min, *i.e.* slow pyrolysis regime. The system was left to cool under N₂/H₂ mixture. The Biochar@Ag weight was found to be ~0.44 g corresponding to a yield of ~37 %.

The same agrowaste, without any silver nitrate, was pyrolyzed and the pyrolysis yield was found to be ~26 %.

2.2. Characterization of Biochar materials

X-ray diffraction (XRD) was used for structural characterization using a D8 Advance Bruker diffractometer (Cu K α radiation). Data were acquired in the 5-80 ° 2 θ range (step size = 0.01 °) using an incident wavelength λ of 1.54056 Å.

XPS analysis of Biochar@Ag was performed using a NEXSA apparatus (Thermo), fitted with monochromated X-ray beam and operated in the constant analyzer energy mode. The pass energy was set to 200 and 80 eV for the survey and narrow regions, respectively. A flood gun was employed to compensate for the static charge buildup.

SEM images and EDX spectra were obtained with a Zeiss Merlin Field Emission scanning electron microscope (Oberkochen, Germany), operated at 5 kV and coupled with a SDD X-Max from Oxford Instruments. The biochar samples were coated with a 3 nm-thin layer of

palladium in order to avoid static charge. Palladium was deposited using a Cressington 208HR sputter-coater coupled with a Cressington MTM-20 thickness controller.

Thermogravimetric analyses were conducted using a Setaram machine (Setsys Evolution model). The samples were heated up from RT to 800 °C, in air, at a heat rate of 10 °C/min.

2.3. *In vitro* Leishmanicidal and trypanocidal assays of Biochar@Ag

2.3.1. Parasite strains

The anti-kinetoplastid activity of Biochar and Biochar@Ag was evaluated against the promastigote stage of *Leishmania donovani* (MHOM/IN/90/GE1F8R) and *Leishmania amazonensis* (MHOM/BR/77/LTB0016) and epimastigote form of *Trypanosoma cruzi* (Y strain).

2.3.2. *In vitro* leishmanicidal effect

The *in vitro* assay was performed using the alamarBlue® method as previously described (paper atteneri). This simple and rapid test is based on the reduction of non-fluorescent rezasurin into fluorescent resorufin by viable cells. This reaction could be measured by colorimetric or fluorometric sensor. Both tested nanoparticle's Biochar and Biochar@Ag were resuspended in physiologic water at a suitable concentration. In Further serial dilutions using *Leishmania* medium (RPMI 1640) were made in a sterilized 96-wellmicrotiter plates (Corning™) to get a final volume of 100 µL per well. Later, 100 µL of *Leishmania donovani* or *Leishmania amazonensis* were added to each well, at a concentration of 2×10^6 cells/mL. Finally, 20 µL of alamarBlue® reactant were added to the entire plate. After an incubation of 72 h, the plate was checked up visually using an inverted microscope and the emitted fluorescence was measured with an EnSpire® Multimode Plate Reader (Perkin Elmer, Madrid, Spain) at 570/585 nm. Leishmanicidal activity was expressed as IC₅₀ values (the concentration of a sample which caused a 50 % reduction in parasite viability). Those values were calculated by non-linear regression analysis.

2.3.3. *In vitro* evaluation against epimastigotes of *Trypanosoma cruzi*

The nanoparticles were tested against the epimastigotes of *T. cruzi*. Briefly, in 96-well plates samples resuspend in physiological water were serially diluted in 100 µL of LIT medium supplemented with 10 % heat-inactivated fetal bovine serum. In all tests. Later, epimastigotes

in logarithmic growth phase were counted using the Invitrogen Tali Image-based Cytometer, adjusted to 10^6 cells/mL, and 100 μ L were added to the 96-well plate. Finally, 20 μ L of alamarBlue® reactive were added to the entire plate to be incubated at 27 °C for 72 h. The plate was observed under an inverted microscope after 72 h of incubation and analyzed statistically as described in the leishmanicidal test.

2.4. Cytotoxicity Assay

The cytotoxicity assay was performed as described in literature [3]. Briefly, 2×10^5 of macrophages cells were seeded in a 96-well plate in a 5 % CO₂ incubator at 37 °C. Cells were allowed to adhere in 20 min. Meanwhile, serial dilutions of the Biochar@Ag were prepared in a sterile deep well plate; later 50 μ L of each concentration were added to the macrophage 96 well plate. Finally, the alamarBlue® Reagent was added into each well at an amount equal to 10% of the medium volume and the plate was incubated for 24 hours at 37°C with 5 % CO₂ atmosphere. The percentage of cell viability was evaluated using the alamarBlue® assay. Dose response curves were plotted and the CC₅₀ values were calculated. Statistical analysis: all data are expressed as the mean \pm standard deviation of at least three independent experiments. To highlight the dose response effect of the Biochar@Ag, a statistical comparison was conducted using one-way analysis of variance (ANOVA). All analyses and graphics were done by GraphPad Prism version 9.0. Statistical significance was set at $p < 0.05$.

3. Results and Discussion

3.1. Strategy of Biochar@Ag design and antiparasitic application

There are numerous ways to prepare metallic nanoparticle-loaded biochar. The direct method consists in impregnating the biomass precursor with silver nitrate followed by pyrolysis. The indirect method, consists in making biochar first then react with metal ions for the in situ deposition of the latter and their subsequent reduction into biochar-supported metallic nanoparticles. Of relevance to this work, Huang et al. [18] treated silver nitrate with KOH to obtain AgO, and added rosin. The mixture was pyrolyzed at 400 °C for 8 min under air. In this work, we avoid the use of KOH or any acid treatment or post-treatment of the biochar. We have pyrolyzed silver nitrate-impregnated olive stone powder particles in the slow pyrolysis regime, at 400 °C for 15 min and the resulting material was tested for antiparasitic activity in comparison to bare biochar. Figure 1 depicts the whole strategy of the work.

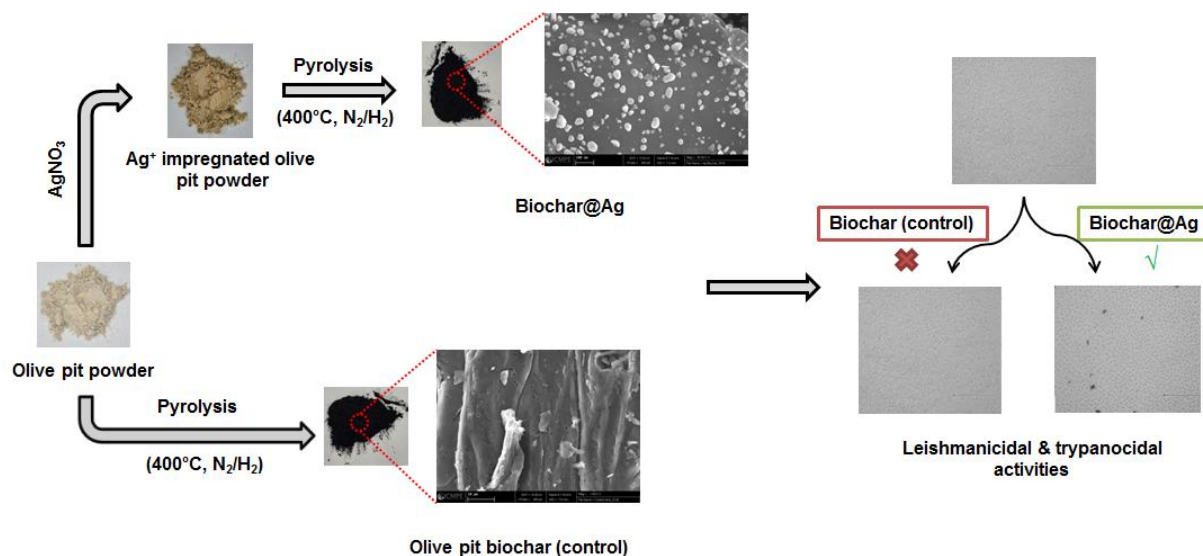


Figure 1. General procedure for making silver nanoparticle-loaded biochar for anti-kinetoplastid application.

3.2. Physicochemical properties of Biochar and Biochar@Ag

Figure 2 displays the XRD patterns of Biochar@Ag and the reference bare Biochar. The latter is amorphous and exhibits no diffraction peaks. In contrast, sharp diffraction peaks are noted for Biochar@Ag; they are centred at $2\theta = 37.9, 44.0, 64.3$ and 77.2° and assigned to Ag(111), Ag(200), Ag (220) and Ag(311) crystallographic planes, respectively. This is in line with results reported elsewhere for silver NP-loaded rosin biochar prepared carbonization of rosin modified with KOH-treated silver nitrate [18]. The XRD pattern of Biochar@Ag is consistent with pure metallic silver nanoparticles loaded on biochar.

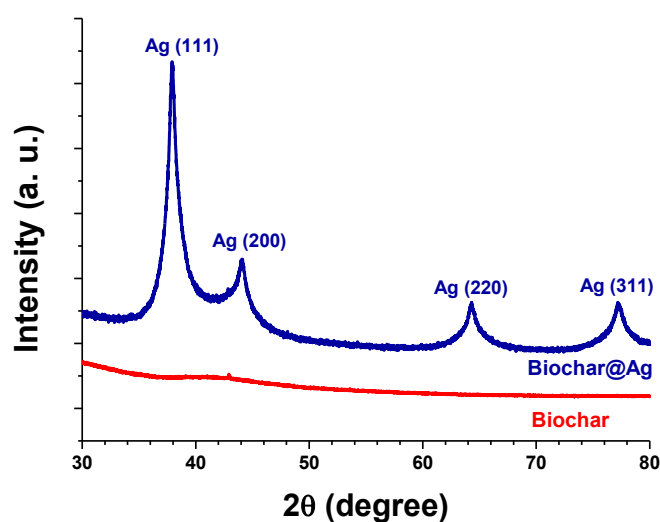


Figure 2. XRD patterns of bare Biochar and Biochar@Ag composite.

XP spectra and surface elemental composition of Biochar@Ag are displayed in Figure 3. The survey region (Figure 3a) exhibits sharp Ag3d doublet is noted with Ag3d_{5/2} and Ag3d_{3/2} peaks centred at 368.2 and 374.2 eV, respectively (Figure 3b). These binding energy values [19] and 6 eV splitting [20] are consistent with silver in the metallic state. C1s narrow region from the biochar is displayed in Figure 3c; it is peak fitted with four components assigned to sp² carbon atoms (284.6 eV), sp³ carbon atoms (285.3 eV), C-O (286.8 eV) and O-C=O (288.6 eV) carbon atom types [21]. Figure 3d depicts the surface elemental composition (in at. %); O/C ratio is about 0.16, lower than 0.20 obtained for *Shorea robusta* leaves, carbonized at 300 °C [20]. A lower pyrolysis temperature induces less degradation of the cellulosic initial material and thus leads to higher O/C ratio as is the case in the case of *S. robusta* [20]. One interesting point is that the actual surface silver content is high, and parallels the sharp Ag3d doublet noticed in Figure 3a. This indicates that direct pyrolysis of silver nitrate-impregnated biomass is an effective way to obtain high silver nanoparticle loading on biochar, compared to the impregnation of biochar with pre-fabricated silver nanoparticles. Indeed, the survey region reported by Shaikh *et al.* [20] exhibits a very low relative intensity of the Ag3d doublet.

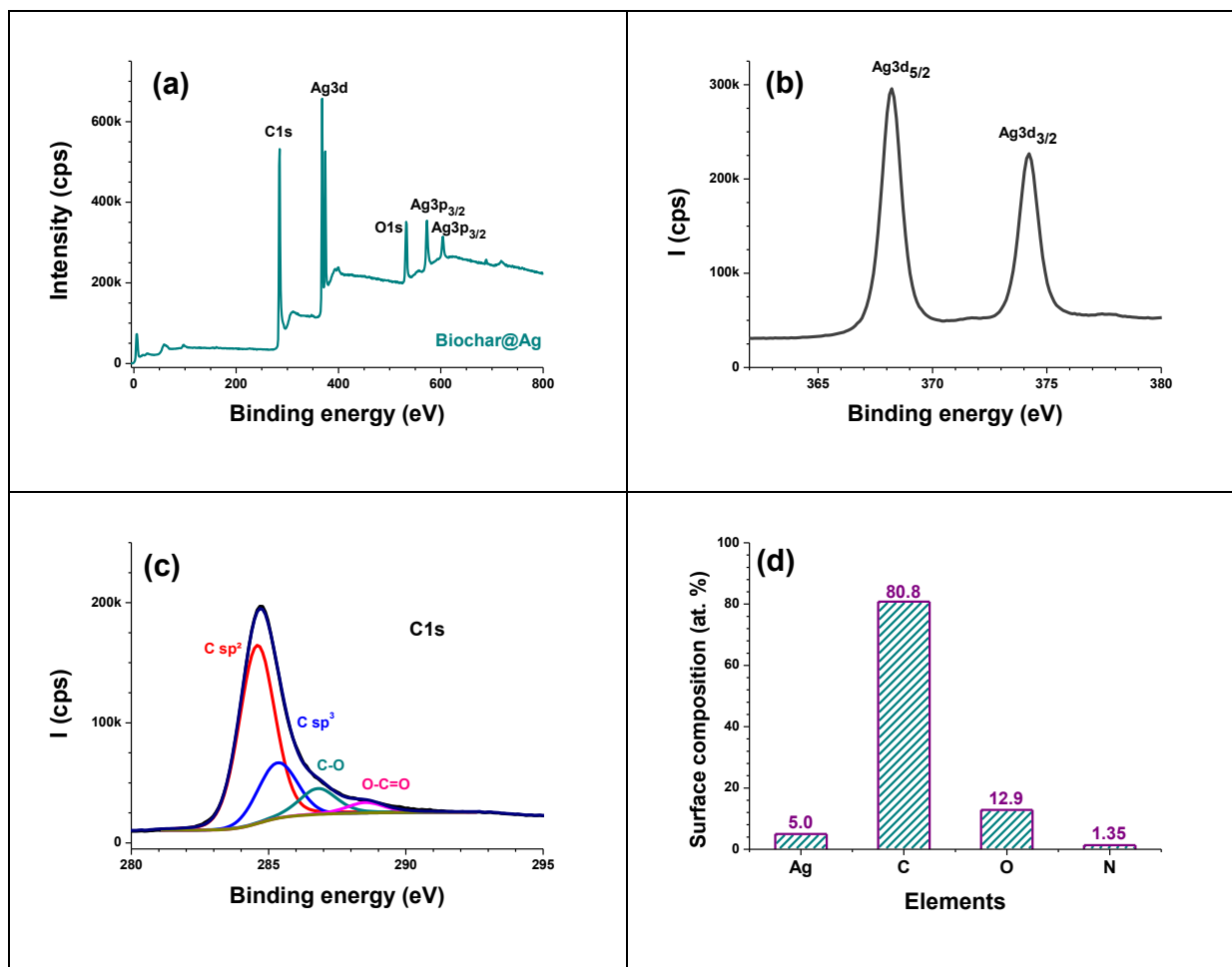


Figure 3. XPS spectra and composition of Biochar@Ag: (a) survey, (b) Ag3d, (c) C1s, and (d) chemical composition in at.%.

SEM/EDX can further give credit to the XPS analysis and could explain the sharp Ag3d peak. Figure 4 displays SEM/EDX analyses of Biochar and Biochar@Ag. One can clearly note that very dense distribution of silver nanoparticles (Figures 4d,e) over the biochar microparticles, which have almost a wax-shaped structure (Figure 4a,b). No particular feature is noted for Biochar at higher magnification (Figure 4c), which contrasts with the individual or stacked, triangular silver nanoparticles (68 ± 7 nm) displayed in Figure 4g for Biochar@Ag. It is also worth to note the uniform distribution of the Ag NPs (Figure 4f), which fully credits the effective simple impregnation approach devised in this work. Prominent Ag peak is noted in Figure 4h for Biochar@Ag compared to Figure 4d showing the absence of any Ag peak for the bare Biochar. The Ag/C ratio is ~ 0.04 and ~ 0.06 as determined by EDX (Figure 4h) and by XPS, respectively. This is an expected trend as XPS is more surface specific than EDX.

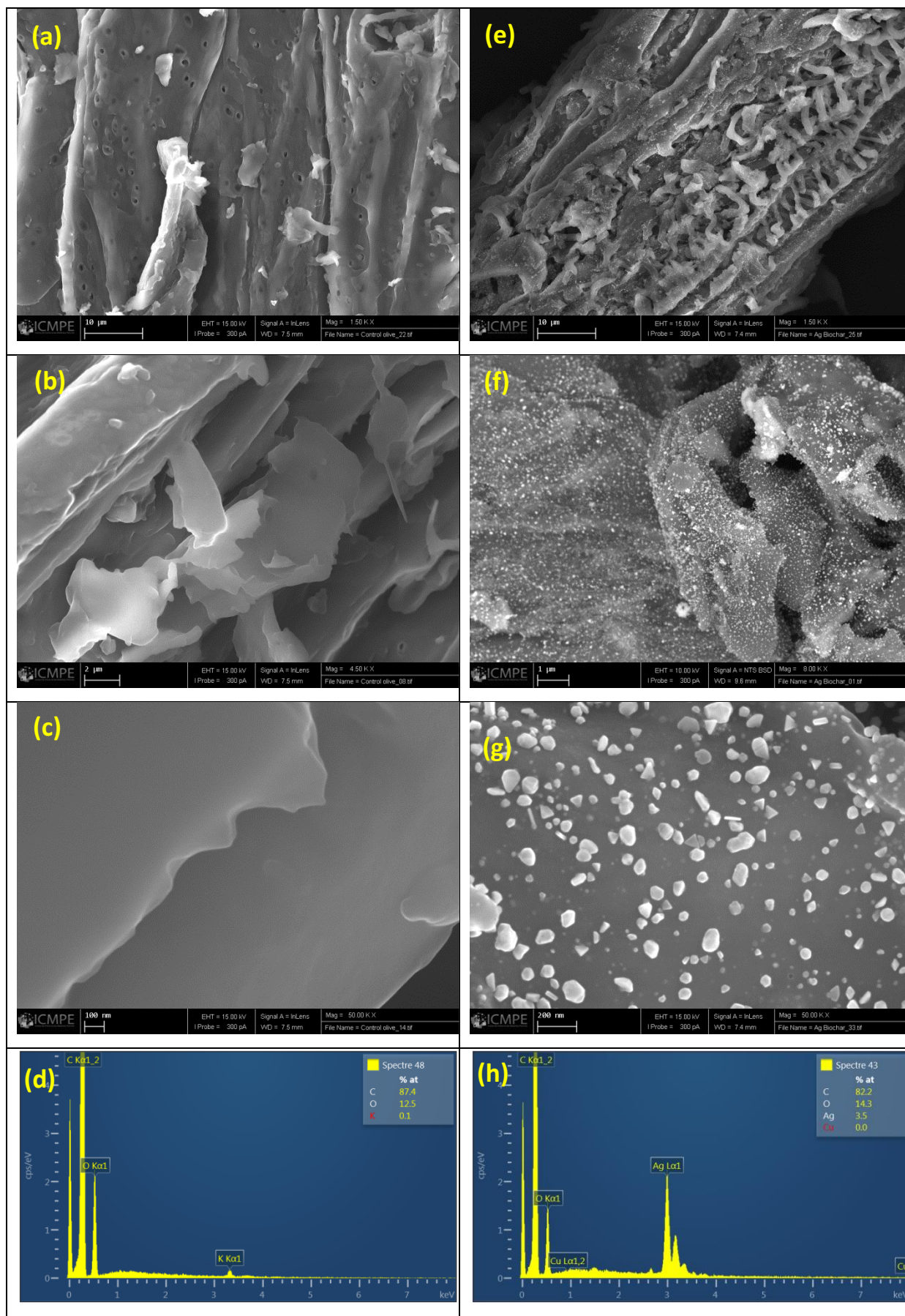


Figure 4. SEM (a-c, e-g) and EDX (d,h) analyses of Biochar (a-d) and Biochar@Ag (e-h) at various magnification. EDX spectra in d and h are representative of all EDX analyses.

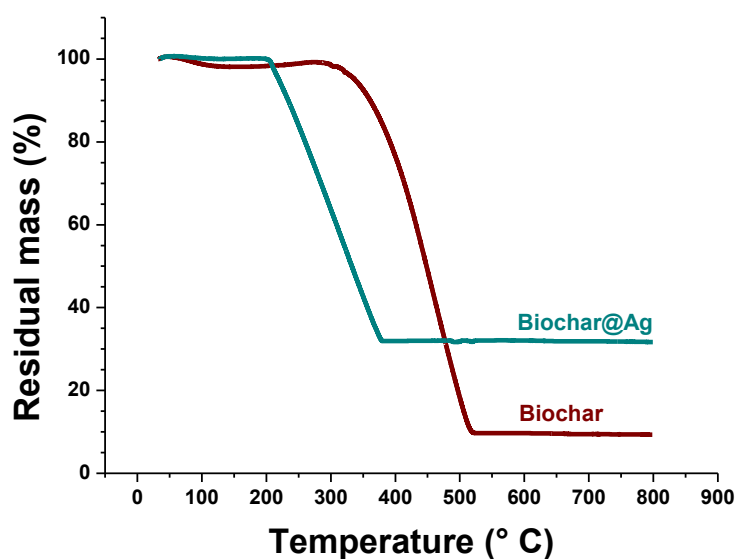


Figure 5. TGA analyses of Biochar and Biochar@Ag.

Figure 5 plots the thermograms of Biochar@Ag and the reference bare Biochar. The gravimetric measurements were performed under air in order to burn out the biochar; this is the reason for low residual 9.7 wt. %. In the case of Biochar@Ag, the higher residual mass (31.5 %). The onset of Biochar degradation is 274 °C, higher than that of Biochar@Ag which starts to degrade at 200 °C, well below the bare Biochar. This could be due to catalytic thermal degradation of the carbonized matter by silver NPs [22]. Degradation progresses until 377 °C and the mass becomes stable. In the case of Biochar, thermal degradation keeps progressing until reaching 522 °C the onset of stable Biochar weight loss.

3.3. Antikinetoplastid activities

Table 1. Summary of IC₅₀ and CC₅₀ values obtained *in vitro*

	<i>Trypanosoma cruzi</i> IC ₅₀	<i>Leishmania donovani</i> IC ₅₀	<i>Leishmania amazonensis</i> IC ₅₀	<i>Murine Macophages</i> CC ₅₀
Biochar@Ag (ppm)	12.154 ± 0.206 ^b	9.942 ± 0.900 ^a	14.555 ± 1.035 ^c	70.33 ± 0.550
Benznidazole (µM)	6.940 ± 1.940	NT	NT	> 400 µM
Miltefosine (µM)	NT	3.32 ± 0.27	6.48 ± 0.24	72.190 ± 3.060

* Means within strains with different lower-case letters (a–c) are significantly different ($p < 0.05$).

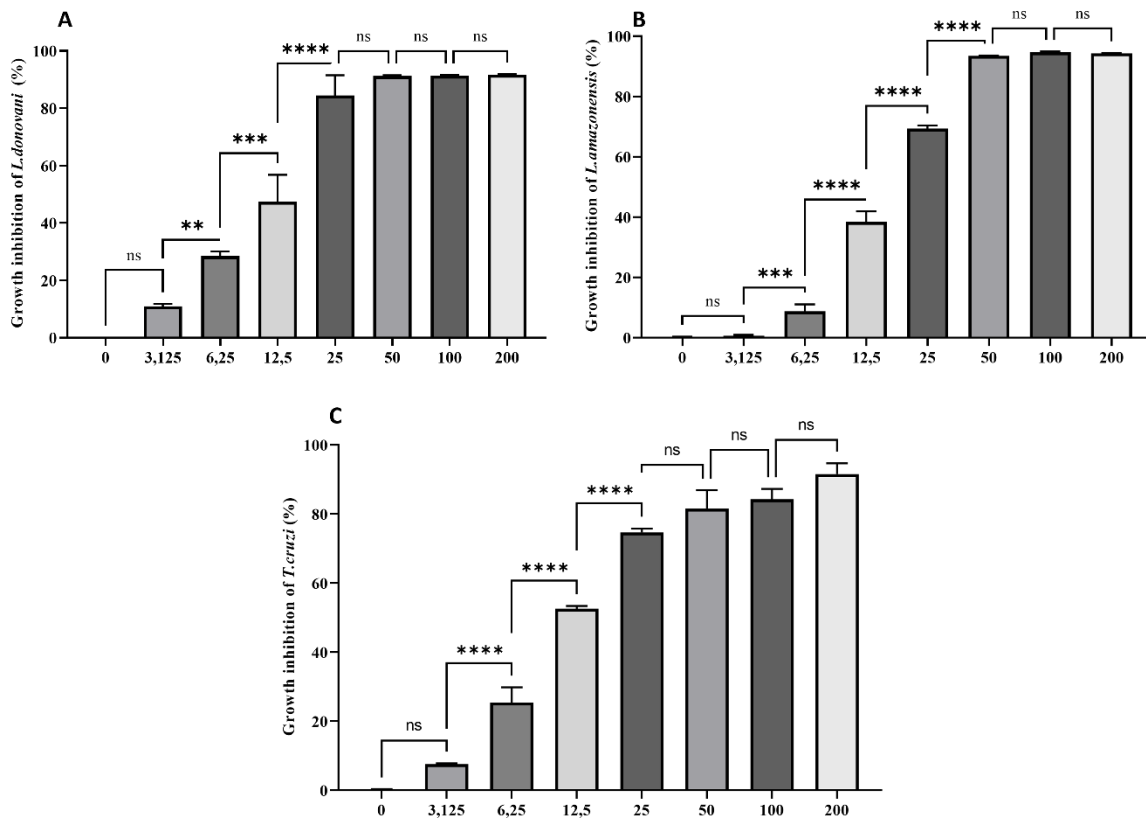


Figure 6. Effect of the Biochar@Ag on promastigote stage of *L. donovani* (A), *L. amazonensis* (B) and *Trypanosoma cruzi* (C). The bar graph includes the calculated percentage of growth inhibition. Differences between the values were assessed using one-way analysis of variance (ANOVA). Data are presented as means \pm SD (N = 3) ** p < 0.01; *** p < 0.001; **** p < 0.0001.

Leishmanicidal and trypanocidal activities of Biochar and Biochar@Ag were determined using almarBlue® method. The assay was done against promastigotes stage of *L. amazonensis* and *L. donovani* and epimastigotes of *T. cruzi*. The obtained values of concentrations inhibiting 50% of the parasite (IC₅₀) are summarized in Table 1. The antiprotozoal activity was dose dependent as illustrated in the Figure 6. The natural Biochar was inactive against all the tested strains. In contrast, Biochar@Ag was very effective to inhibit all the strains with IC₅₀ of 12.154 ± 0.206 , $9,942 \pm 0.900$ and 14.555 ± 1.035 ppm against *T. cruzi*, *L. donovani* and *L. amazonensis*, respectively. The ANOVA analysis revealed that the antikinoplastid capacity was statistically affected by the dose and the type of parasite used. Indeed, the most sensitive parasite was *L. donovani* where a concentration of 25 ppm was able to inhibit 90% of the initial cell culture (Figure 7C and 7D), whereas a concentration of 50 ppm was needed to inhibit 90% of *Trypanosoma cruzi* (7E and 7F) and *Leishmania amazonensis* (Figure 7A, B). On the other hand, the toxicity of the nanoparticles

was evaluated towards murine macrophages and the cytotoxic concentration at 50% was determined. The CC_{50} of the Biochar@Ag was 70.33 ± 0.550 .

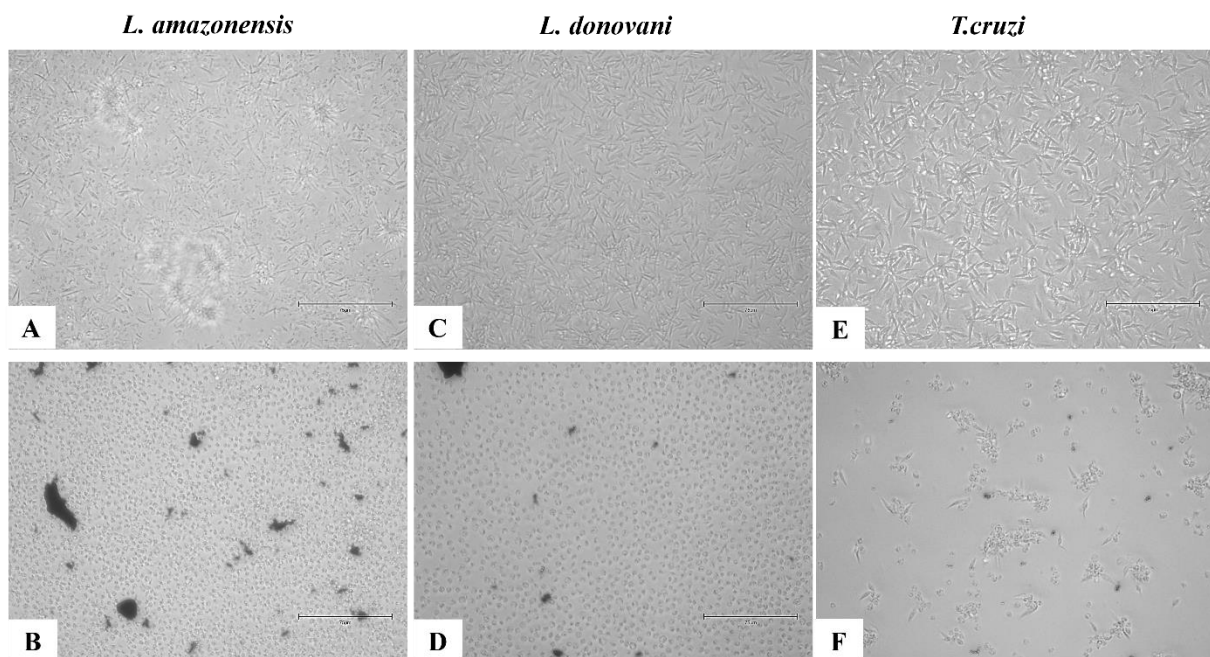


Figure 7. Effect of Biochar@Ag on *Leishmania amazonensis* at 25ppm; *Leishmania donovani* at 12.5 ppm (D) and *Trypanosoma cruzi* at 25 ppm (F). Negative control for each strains (A, C and E). Images (40X) are representative of the cell population observed in the performed experiments. Images were obtained using an EVOS FL Cell Imaging System AMF4300, Life Technologies, USA. Scale bar = 75 μ m.

Conclusion

To sum up, we have prepared silver nanoparticle-loaded biochar (Biochar@Ag) by pyrolysis of silver nitrate –impregnated olive pit powder at 400 °C for 15 min, in the slow regime (heat rate = 30°C/min). Dense and even distribution of triangular silver NPs was noted by SEM, which accounts for very sharp Ag3d peaks recorded by XPS surface analysis. A more porous structure was observed for Biochar@Ag compared to bare Biochar, possibly implying an effect of silver nanoparticles which catalyze the degradation of the biomass or alter its structure during pyrolysis. A concentration of 50 ppm of Biochar@Ag was able to eliminate 90% of three different kinetoplastid including *Leishmania donovani*, causative organism of kala-azar and visceral leishmaniasis, *Leishmania amazonensis*, causative agent of cutaneous leishmaniasis, and *Trypanosoma cruzi*, causative agent of Chagas disease.

From what has been stated above, we have provided a simple pyrolysis method, in the slow regime, to design antiparasitic application of Biochar@Ag against *L. donovani*, *L. amazonensis* and *T. cruzi* with lower cytotoxic effect on murine macrophage; although further studies are needed to illustrate its action mode on the parasite. This *waste-to-wealth* procedure could be adapted for other anti-tropical parasite applications, and more importantly it could be scaled up given its simplicity, versatility and low-cost.

Acknowledgements

The authors would like to thank both the French and Egyptian Governments for funding AMK's contribution through a fellowship granted by the French Embassy in Egypt (Institut Francais d'Egypte) and Science and Technology Development Fund (STDF)-Egypt, Project number (42248). Wallonie Bruxelles International (WBI) is acknowledged for the provision of a grant "Bourse WBI Excellence World" (No Imputation 101386, Article Budgétaire 33.01.00.07). This study was supported as well by the RICET (project no. RD16/0027/0001 of the programme of Redes Temáticas de Investigación Cooperativa, FIS), CIBER de Enfermedades Infecciosas (CIBERINFEC), Instituto de Salud Carlos III (CB21/13/00100) and Cabildo de Tenerife 21/0587 cofunded by FDCAN and MEDI (Tenerife Innova Programme).

References

1. Stuart, K., et al., *Kinetoplastids: related protozoan pathogens, different diseases*. The Journal of clinical investigation, 2008. **118**(4): p. 1301-1310.
2. Lin, C., et al., *N6-modification of 7-Deazapurine nucleoside analogues as Anti-Trypanosoma cruzi and anti-Leishmania agents: Structure-activity relationship exploration and In vivo evaluation*. European Journal of Medicinal Chemistry, 2022: p. 114165.
3. de Fuentes-Vicente, J.A., et al., *What makes an effective Chagas disease vector? Factors underlying Trypanosoma cruzi-triatomine interactions*. Acta Tropica, 2018. **183**: p. 23-31.
4. Villalta, F., et al., *VNI cures acute and chronic experimental Chagas disease*. The Journal of infectious diseases, 2013. **208**(3): p. 504-511.
5. Rassi, A. and J.M. de Rezende, *American trypanosomiasis (Chagas disease)*. Infectious Disease Clinics, 2012. **26**(2): p. 275-291.
6. Allahverdiyev, A.M., et al., *Antileishmanial effect of silver nanoparticles and their enhanced antiparasitic activity under ultraviolet light*. International journal of Nanomedicine, 2011. **6**: p. 2705.
7. Lima, D.d.S., et al., *Chitosan-based silver nanoparticles: A study of the antibacterial, antileishmanial and cytotoxic effects*. Journal of Bioactive and Compatible Polymers, 2017. **32**(4): p. 397-410.
8. Ghosh, S., et al., *Dioscorea bulbifera mediated synthesis of novel AuCoreAgshell nanoparticles with potent antibiofilm and antileishmanial activity*. Journal of Nanomaterials, 2015. **2015**.
9. Abamor, E.S., et al., *Meglumine antimoniate-TiO₂@ Ag nanoparticle combinations reduce toxicity of the drug while enhancing its antileishmanial effect*. Acta tropica, 2017. **169**: p. 30-42.
10. Alti, D., et al., *Gold-Silver Bimetallic Nanoparticles Reduced with Herbal Leaf Extracts Induce ROS-Mediated Death in Both Promastigote and Amastigote Stages of Leishmania donovani*. ACS omega, 2020. **5**(26): p. 16238-16245.
11. Espuri, P.F., et al., *Synthesis and evaluation of the antileishmanial activity of silver compounds containing imidazolidine-2-thione*. JBIC Journal of Biological Inorganic Chemistry, 2019. **24**(3): p. 419-432.
12. Jebali, A. and B. Kazemi, *Nano-based antileishmanial agents: a toxicological study on nanoparticles for future treatment of cutaneous leishmaniasis*. Toxicology in vitro, 2013. **27**(6): p. 1896-1904.

13. Almayouf, M.A., et al., *The effects of silver nanoparticles biosynthesized using fig and olive extracts on cutaneous leishmaniasis-induced inflammation in female balb/c mice*. Bioscience Reports, 2020. **40**(12): p. BSR20202672.
14. Gedda, M.R., et al., *Evaluation of safety and Antileishmanial efficacy of amine functionalized carbon-based composite nanoparticle appended with amphotericin B: An in vitro and preclinical study*. Frontiers in chemistry, 2020. **8**: p. 510.
15. Silva Viana, R.L., et al., *Green synthesis of antileishmanial and antifungal silver nanoparticles using corn cob xylan as a reducing and stabilizing agent*. Biomolecules, 2020. **10**(9): p. 1235.
16. Chopra, I., *The increasing use of silver-based products as antimicrobial agents: a useful development or a cause for concern?* Journal of antimicrobial Chemotherapy, 2007. **59**(4): p. 587-590.
17. Yildizli, G., G. Coral, and F. Ayaz, *Biochar as a Biocompatible Mild Anti-Inflammatory Supplement for Animal Feed and Agricultural Fields*. Chemistry & biodiversity, 2021.
18. Huang, J.-F., et al., *Facile pyrolysis preparation of rosin-derived biochar for supporting silver nanoparticles with antibacterial activity*. Composites Science and Technology, 2017. **145**: p. 89-95.
19. Abbas, Q., et al., *Biochar-induced immobilization and transformation of silver-nanoparticles affect growth, intracellular-radicals generation and nutrients assimilation by reducing oxidative stress in maize*. Journal of hazardous materials, 2020. **390**: p. 121976.
20. Shaikh, W.A., R.U. Islam, and S. Chakraborty, *Stable silver nanoparticle doped mesoporous biochar-based nanocomposite for efficient removal of toxic dyes*. Journal of environmental chemical engineering, 2021. **9**(1): p. 104982.
21. Kim, D.-G. and S.-O. Ko, *Effects of thermal modification of a biochar on persulfate activation and mechanisms of catalytic degradation of a pharmaceutical*. Chemical Engineering Journal, 2020. **399**: p. 125377.
22. Giudicianni, P., et al., *Inherent metal elements in biomass pyrolysis: A review*. Energy & Fuels, 2021. **35**(7): p. 5407-5478.